### Thermonuclear neutrons

The neutron yield of the z-pinch experiment was monitored by time-of-flight scintillation counters that measured neutron velocities and by activation detectors that measured the total neutron yield integrated over time. The energy distribution of neutrons from thermonuclear DD fusion peaks at 2.45 MeV, and its width increases with the ion temperature.

Figure 3 shows the time delay between the neutron signals at two counters whose distances from the imploding capsule differ by 98 cm. The delay yields a peak neutron energy of $2.46 \pm 0.15$ MeV, and the distribution has the expected shape for a thermonuclear burn plus some scattering in the experiment's shielding. Furthermore, the measured total neutron yield, $(3.0 \pm 1.3) \times 10^{10}$, was in reasonable agreement with computer simulations of the imploding deuterium capsule. So were the argon spectral measurements.

Nonetheless, it is important to distinguish carefully between a true thermonuclear neutron yield—that is, fusion events in which thermal kinetic energy overcomes the DD Coulomb repulsion—from uninteresting "ion-beam" fusion events attributable to the kinetic energy of deuterons accelerated toward the hohlraum's bottom electrode. To that end, the group looked for a telltale enhancement of the neutron yield in the downward direction. And they looked for a neutron yield from a z-pinch shot (the yellow trace in figure 3) in which the capsule was spiked with enough xenon to keep the ion temperature well below threshold for significant thermonuclear fusion. The negative results of both tests convinced the group that any non-thermonuclear contribution to the neutron yield was negligible.

Scaling up the dynamic-hohlraum pulsed-power technology to the requirements for a useful reactor raises many questions yet to be confronted. That's also true, of course, for all the other fusion-power schemes. At the Z Machine, the fuel capsule has to sit much closer to the machine's hardware than it does at the NIF. It's not a problem in a laboratory, where experimental shots are few and far between. But for a power plant, this crowding raises the problem of excessive neutron activation. And there's the problem of damage to the transmission lines at high repetition rates.

With regard to energy efficiency, the Z Machine, an experimental facility still far from any reactor design, delivers to the hohlraum about 15% percent of the energy it takes from the electric grid. For laser ICF, it seems possible to build high-power diode-driven lasers with efficiencies as high as 10%, but they might be prohibitively expensive. High capital cost is also a challenge for yet another ICF alternative: heavy-ion beams.

"It's much too early to declare a winner in the quest for a useful ICF technology," says Thomas Mehlhorn, head of Sandia's dynamic-hohlraum program, "but at least we're now in the game."

**Bertram Schwarzschild**

### References


1. J. Bailey et al., *Phys. Rev. Lett.* **89**, 095004 (2002).
2. J. Bailey et al., http://arXiv.org/abs/physics/0306039.
3. S. Slutz et al., *Phys. Plasmas* **10**, 1875 (2003).


# New Atomic Magnetometer Achieves Subfemtotesla Sensitivity

**In a field dominated by superconducting quantum interference devices (SQUIDs), a rival technique has gotten a boost by operating in a new parameter regime.**

Measuring small magnetic fields plays an important role in many areas of physics. Mapping small variations in Earth's magnetic field, tracing the history of geodynamo reversals as recorded in ancient rocks, characterizing new superconductors and other materials, searching for deviations from the standard model of particle physics, mapping the fields and currents of heart or brain activity—all require precise measurements of magnetic fields that are orders of magnitude smaller than Earth's.

A key benchmark in such applications is a device's sensitivity—the square root of the mean square field noise per unit bandwidth of the device. The device front-runner in most magnetometry applications is the superconducting quantum interference device (SQUID). Formed from superconducting rings interrupted by Josephson junctions, SQUID magnetometers for applications such as

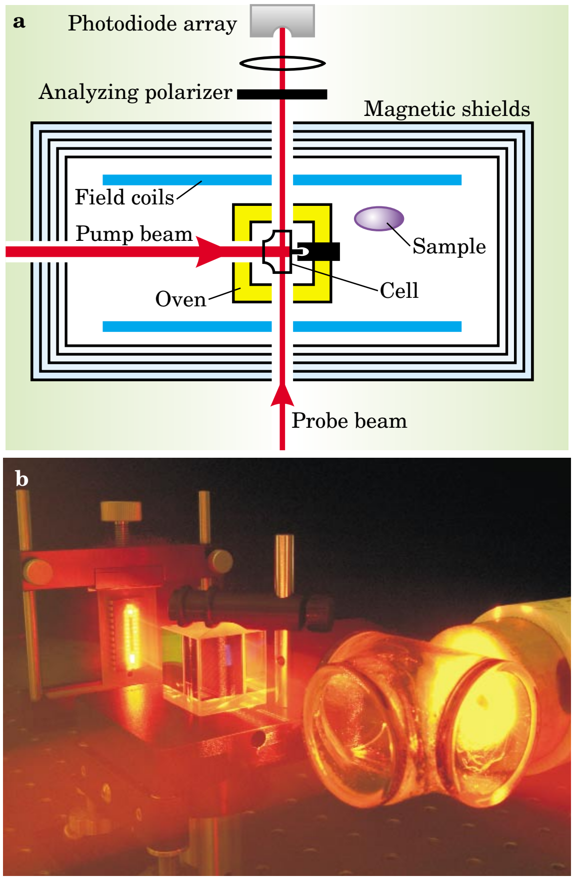


**Figure 1. Experimental** setup of an atomic magnetometer with subfemtotesla sensitivity. **(a)** This schematic illustrates the major components. A T-shaped cell, 3 cm × 3 cm × 4 cm, contains potassium metal along with helium and nitrogen buffer gases. The cell is heated to generate a potassium vapor. The spins of the unpaired electrons in the vapor are oriented by a circularly polarized pump laser. A linearly polarized probe beam, which passes through the cell and a polarization analyzer before reaching an array of photodiodes, detects the effect on the vapor's magnetization of the magnetic field from a nearby sample. Magnetic shields and electromagnet coils around the cell and sample reduce the ambient magnetic field by six orders of magnitude for better sensitivity. (Adapted from ref. 1.) **(b)** A picture of the apparatus with the oven, coils, and shields removed.

magnetoencephalography have sensitivities of around 1 fT/Hz$^{1/2}$. Their input coils, which couple magnetic flux to the superconducting ring, can be fabricated in different geometries to fashion gradiometers insensitive to background magnetic fields. The use of high-temperature superconductors permits operation at liquid-nitrogen temperature (77 K), but the best sensitivities to date have been obtained with low-temperature superconductors at liquid-helium temperature (4 K).

Another class of sensitive magnetometers, which has been around for more than 40 years, exploits the effects of magnetic fields on the unpaired spins of individual atoms. Atomic magnetometers have achieved sensitivities comparable to SQUIDs, but at a price: They are large, which reduces their spatial resolution and limits their usefulness for magnetic imaging applications.

Now, Michael Romalis and colleagues from Princeton University and from the University of Washington in Seattle have demonstrated a new atomic magnetometer that achieves subfemtotesla sensitivity with high spatial resolution.[1] "This combination of high sensitivity and good spatial resolution is a real breakthrough," says Dmitry Budker of the University of California, Berkeley.

## Measuring the Zeeman splitting

Atomic magnetometers measure, in various ways, the Zeeman effect: the magnetic-field-induced shift of the energy levels of an atom's spin states. Alkali atoms, such as rubidium and potassium, are most commonly used because their single unpaired electron makes for a simple spin-½ system. Bulk alkali metal placed in a magnetometer will generate a vapor whose density depends on the operating temperature.

To get a vapor magnetization large enough to measure, atomic magnetometers optically pump the gaseous atoms into a polarized state. Romalis and coworkers use circularly polarized light for pumping; some other magnetometers use linearly polarized light. The light's frequency is resonant with the transition from the atom's ground state to a higher, excited state. In the case of circularly polarized light, angular momentum conservation allows only electrons in one spin state to absorb photons. But the excited state can relax back to either spin orientation in the ground state. The net effect of the pumping process is a depletion of the population in the ground spin state that couples to the light. The resulting spin polarization is appreciable and can, for some magnetometers, approach 100%.

Many different styles of atomic magnetometers have been developed. One approach, championed by Eugene Alexandrov at the Vavilov State Optical Institute in St. Petersburg, Russia, is a double-resonance technique that combines optical pumping with radio-frequency radiation.[2] When the alkali vapor is fully polarized, no electrons are in the appropriate spin state to absorb a photon, and the optical pumping beam is fully transmitted. If an RF field is applied to the magnetometer and the frequency is swept, the vapor becomes depolarized when the frequency is resonant with the Zeeman splitting of the ground-state, and the intensity of the transmitted light drops. The frequency at which the drop occurs is a measure of the magnetic field strength. Such magnetometers have attained sensitivities approaching 1 fT/Hz$^{1/2}$, and magnetometers based on the double-resonance technique are commercially available.

Robert Wynands and colleagues at the University of Fribourg in Switzerland have recently used two double-resonance magnetometers, configured as a gradiometer, for magnetocardiography—the mapping of the heart's magnetic field.[3] One magnetometer was rastered near the heart to measure the 100-pT field it produced; the other magnetometer was farther away and was used to measure and subtract stray fields. The measurement sensitivity was about 100 fT/Hz$^{1/2}$.

Another approach used by Wynands and coworkers for atomic magnetometry is based on a phenomenon known as coherent population trapping (CPT).[4] Two lasers are used to excite transitions from different hyperfine levels of the ground state to a common excited state. When the lasers are properly tuned to the field-dependent energy levels, they drive the electrons into a coherent superposition of the two hyperfine states—a so-called dark state that doesn't couple to either laser. The resulting trough in the atoms' absorption spectrum is very narrow and thus provides a sensitive determination of the magnetic field: This technique has achieved sensitivities around 1 pT/Hz$^{1/2}$.

In yet another approach, developed by Budker and coworkers, a single beam of linearly polarized light both pumps the magnetometer and probes its polarization. The detection technique, which utilizes nonlinear magneto-optical rotation, has a theoretical sensitivity limit of 0.3 $\mathrm{fT/Hz}^{1/2}$, and its dynamic range can be expanded to include fields on the order of Earth's.[5]

The sensitivities of atomic magnetometers can be limited by the lifetime of the spin coherence—the $T_2$ in magnetic resonance terms. A limiting factor in atomic magnetometers is often spin-exchange collisions. When two atoms collide, angular momentum can be transferred from one spin to another. Although that process conserves angular momentum, such collisions are still a problem, because they can switch atoms between different hyperfine states. Electrons precess in opposite directions in the two states, and thus they lose coherence.

Most atomic magnetometers operate at a vapor density low enough for the line broadening due to spin-exchange collisions to be tolerable. But spin exchange need not be a liability. In the 1970s, Will Happer (now at Princeton) and colleagues considered the limiting case of very low magnetic field and high vapor density. In that regime, the spin exchange rate is much larger than the precession frequency; the more frequent the collisions are, the more slowly the phases of the different spin states diffuse from each other, and thus, in that limit, the vapor remains polarized.[6] The net effect of spin exchange is merely to slow down the precession slightly. Capitalizing on the reduced decoherence rate in that regime, Romalis and coworkers have demonstrated a sensitivity of 0.54 $\mathrm{fT/Hz}^{1/2}$.

## High sensitivity, low volume

Figure 1 shows the experimental setup used by Romalis and company. A glass cell containing potassium metal is heated by hot air in an oven to 180°C to generate a potassium vapor density of $6 \times 10^{13}$ atoms/$\mathrm{cm}^3$—about four orders of magnitude larger than the typical density of other magnetometers. Circularly polarized light from a 1-mW broadband diode laser optically pumps the vapor, while a second, orthogonal single-frequency laser beam probes the polarization. The probe beam is detuned from resonance to avoid additional optical pumping.

Whereas many atomic magnetometers are scalar—that is, they measure the magnitude of the magnetic field, whatever its direction—this one is a vector magnetometer. Romalis and coworkers configured it to be sensitive only to the component of the magnetic field that's perpendicular to both the pump and the probe beams. When both the collision frequency and the polarization are high, the spin precession frequency depends on the polarization.[7] The new magnetometer avoids that potential source of decoherence by operating quasi-statically near zero field. As figure 2 illustrates, the polarization of the optically pumped potassium vapor, initially aligned in the direction of the pump beam (the $z$ direction), is rotated in the $xz$ plane due to the torque from the $y$-component of the magnetic field. The linearly polarized probe beam, traveling in the $x$ direction, undergoes optical rotation as it traverses the cell: The beam's polarization is rotated by an angle proportional to the $x$-component of the spin magnetization. The angle of rotation is effectively detected by passing the probe beam through a linear polarizer: Only the perpendicular polarization induced in the probe beam is detected by the photodiode array.

Atomic magnetometers can be susceptible to another major cause of spin relaxation: collisions with the cell wall. Paraffin coatings are often used to reduce wall-induced spin decoherence; the Princeton–Washington group instead filled their magnetometer cell with several atmospheres of helium-4 buffer gas. At that pressure, the diffusion of potassium atoms is severely reduced, so that the atoms typically diffuse only a few millimeters during the polarization lifetime.

The short diffusion length has another important benefit: Since the spins drift so little during a measurement, different slices of the magnetometer cell can be used for simultaneous, essentially independent multichannel measurements. The effective volume of the magnetometer is thus only about 0.3 $cm^3$, much smaller than the 1000 $cm^3$ or so typically found for other atomic magnetometers. The photodiode detection array, with seven elements separated by about 3 mm, illustrates the potential of the device: The array provides a one-dimensional map of the magnetic field in the cell. By numerically combining the signals from different channels, background magnetic noise can be rejected, and first- and higher-order field gradients can be obtained.

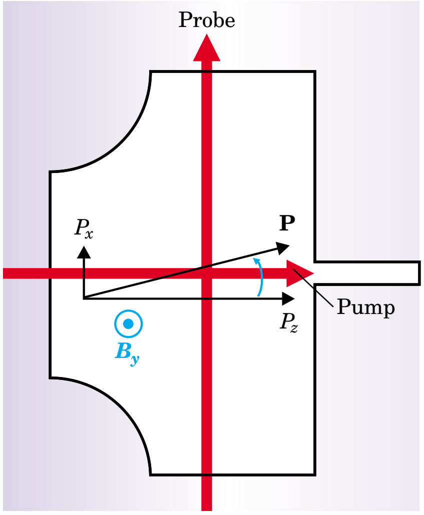


**Figure 2. Optical rotation** is used to measure $B_y$, the component of the magnetic field perpendicular to both the pump and probe laser beams. That field component rotates the potassium polarization **P**, giving it a projection $P_x$ onto the $x$-direction. The polarization angle of the probe beam is rotated by an angle proportional to $P_x$. (Adapted from ref. 1.)

One inescapable constraint of the new magnetometer is that, to be in the requisite limit of fast spin exchange, the background field needs to be very small, well below 100 nanotesla (1 milligauss) or so, orders of magnitude below Earth's field. Screening is therefore required. Furthermore, variations in the laboratory and Earth's field can be on the order of 100 picotesla, and can thus dwarf the extremely small fields sought in the most sensitive experiments. Romalis and company utilized several magnetic shields made of so-called mu-metal, a high-permeability alloy, to screen their experiment from background fields; three orthogonal sets of Helmholtz coils within the shielded enclosure were used to further control the field.

Thermally induced currents in the magnetic shields were the largest source of noise in the initial demonstrations of the magnetometer; they limited the sensitivity to about 0.5 $fT/Hz^{1/2}$. Romalis notes that through optimization—using superconducting magnetic shields, for instance—the magnetometer should be able to get much closer to its theoretical shot-noise sensitivity limit of 0.01 $fT/Hz^{1/2}$.

**Richard Fitzgerald**

## References


1. I. K. Kominis, T. W. Kornack, J. C. Alfred, M. V. Romalis, *Nature* **422**, 596 (2003).
2. See, for example, E. B. Aleksandrov et al., *Laser Physics* **6**, 244 (1996).
3. G. Bison, R. Wynands, A. Weis, *Optics Express* **11**, 904 (2003).
4. C. Affolderbach et al., *Appl. Phys. B* **75**, 605 (2002).
5. D. Budker et al., *Phys. Rev. A* **65**, 055403 (2002).
6. W. Happer, H. Tang, *Phys. Rev. Lett.* **31**, 273 (1973); W. Happer, A. C. Tam, *Phys. Rev. A* **16**, 1877 (1977).
7. J. C. Alfred et al., *Phys. Rev. Lett.* **89**, 130801 (2002).


# Experiments Vindicate a 50-Year-Old Explanation of How Liquid Metals Resist Solidification

**Diffracted x rays reveal a sequence of structural changes in a levitated drop of metal as it cools and freezes.**

A metal's density barely falls on melting. One might guess, therefore, that metal atoms in the liquid phase pack together with almost the same efficiency and with almost the same order as in the solid phase. And—to continue this line of speculation—if one tried to cool a liquid metal below its equilibrium melting point, the few disorderly atoms would easily fall into line with the ordered majority and the liquid would promptly solidify.

In fact, as David Turnbull and Robert Cech showed in 1950, liquid metals can be cooled tens to hundreds of degrees below their equilibrium melting temperatures without solidifying.[1] The trick is to prevent any impurities or other extraneous components from nucleating the nascent solid.

According to classical nucleation theory, a liquid solidifies when thermal fluctuations push it over an energy barrier. This nucleation barrier, $W$, depends on $\Delta G$, the difference between the free energy of the liquid and solid phases. Specifically, $W \propto \Delta G^{-2}$. As a liquid cools, $\Delta G$ increases and lowers the nucleation barrier.

But classical theory also has $W$ proportional to $\gamma^3$, where $\gamma$ is the energy of the interface between the liquid and solid phases. Turnbull and Cech could undercool their samples because, for metals, the interfacial energy is far higher than one might expect based on density alone.

In 1952, to account for the unexpectedly large $\gamma$, Charles Frank put forward a now classic hypothesis.[2] It's